

Supplementary Figure 1

Full alignment of HORMA domain containing proteins (Mad2, Rev7 and Hop1p orthologues) from different organisms

Protein sequences were first aligned using Clustalw (Chenna et al., 2003). The alignment was then manually adjusted and illustrated with the Jalview software (Clamp et al., 2004). Residues laying on Mad2 surface, conserved in the Mad2 family but not in the Rev7 and Hop1 homologues, which were mutagenized in the present study, are shadowed in yellow. Abbreviations for species names are as follow: Mm, *Mus musculus*; Rn, *Rattus norvegicus*; Hs, *Homo sapiens*; Gg, *Gallus gallus*; Xl, *Xenopus laevis*; Dr, *Denio rerio*; Dd, *Dictyostelium discoideum*; Ce, *Caenorabditis elegans*; Dm, *Drosophila melanogaster*; M, *Zea mays*; W, bread wheat; At, *Arabidopsis thaliana*; Sc, *Saccharomyces cerevisiae*; Sp, *Schizosaccharomyces pombe*. Numbering on top of the alignment refers to the HsMad2 sequence.

Supplementary Figure 2

Hydrodynamic properties of Mad2 mutants

(A) Size-exclusion chromatography (SEC) elution profile of bacterially expressed Mad2^{wt} with and without a Cdc20¹¹¹⁻¹³⁸ synthetic peptide. SEC runs were performed on a Superdex-75 column (Amersham) on a Smart system. All 30 μ l fractions spanning from 0.98 to 1.4 ml were separated by SDS-PAGE and stained with Coomassie. Pure recombinant human Mad2^{wt} is a dimer in solution. When this species is mixed with the synthetic peptide encompassing the Mad2-binding-site of Cdc20 (Cdc20¹¹¹⁻¹³⁸), C-Mad2 is formed. This C-Mad2 runs as a monomeric species eluting at approximately 25 KDa (the Cdc20¹¹¹⁻¹³⁸ peptide is too short to influence the elution of Mad2). (B) Mad2^{AC}, a Mad2 deletion mutant lacking the last 10 residues at the C-terminus of Mad2, is locked in the O-Mad2 conformation, is unable to form stable complexes with Mad1 or Cdc20, and elutes as a monomer from a SEC column. Together with the results in (A), this shows

that neither conformer of Mad2 is able to form oligomers if the opposite conformer is missing. (C) Stoichiometric amounts of Cdc20¹¹¹⁻¹³⁸:C-Mad2 and O-Mad2^{AC} were combined and separated by SEC. A trimeric Cdc20¹¹¹⁻¹³⁸:C-Mad2:O-Mad2 complex is formed. The presence of stoichiometric amounts of C-Mad2 and O-Mad2 in this complex is revealed by SDS-page analysis of eluted fractions thanks to the ~1 kDa difference between C-Mad2^{wt} and O-Mad2^{AC}. In summary, pure O-Mad2 or C-Mad2 samples are monomeric and form dimers when mixed stoichiometrically. We have recently suggested that the oligomerization of bacterially expressed HsMad2 is likely due to spontaneous formation of C-Mad2 in the absence of Mad1 or Cdc20, and its consequence binding to O-Mad2 (DeAntoni et al., 2005). (D) The SEC elution profiles of Mad2^{wt}, Mad2^{F141A} and Mad2^{R184A}. At 30 μ M, both mutants behave as monomer in solution, indicating that they are unable to form O-Mad2:C-Mad2 dimers.

Supplementary Figure 3

Hydrodynamic properties of Mad2^{AN15}

(A) SEC runs were performed as described in the legend to Supplementary Figure 2. Bacterially expressed Mad2^{AN15} eluted as expected for a monomeric species from a SEC column (blue trace and upper SDS-PAGE panel). As shown in Supplementary Figure 2, both O-Mad2^{AC} and the C-Mad2^{wt}:Cdc20¹¹¹⁻¹³⁸ complex also elute as monomeric species (given its small size, Cdc20¹¹¹⁻¹³⁸ does not affect significantly the elution of the Mad2^{wt}:Cdc20¹¹¹⁻¹³⁸ complex). When mixed stoichiometrically, O-Mad2^{AC} and Mad2^{AN15} formed a dimeric species, indicating that Mad2^{AN15} is at least predominantly a C-Mad2 conformer of Mad2 (black trace and central SDS-PAGE panel). Note that due to their very small size difference, O-Mad2^{AC} and Mad2^{AN15} could not be resolved by SDS-PAGE. Conversely, Mad2^{AN15} failed to bind the C-Mad2^{wt}:Cdc20¹¹¹⁻¹³⁸ complex, so that both species eluted as expected for monomers (green trace and bottom SDS-PAGE panel). We conclude that Mad2^{AN15} adopts preferentially the C-Mad2 conformation.

on a Superdex-75 column (Amersham) on a Smart system. All 30 μ l fractions spanning from 0.98 to 1.4 ml were separated by SDS-PAGE and stained with Coomassie. Pure recombinant human Mad2^{wt} is a dimer in solution. When this species is mixed with the synthetic peptide encompassing the Mad2-binding-site of Cdc20 (Cdc20¹¹¹⁻¹³⁸), C-Mad2 is formed. This C-Mad2 runs as a monomeric species eluting at approximately 25 KDa (the Cdc20¹¹¹⁻¹³⁸ peptide is too short to influence the elution of Mad2). **(B)** Mad2^{AC}, a Mad2 deletion mutant lacking the last 10 residues at the C-terminus of Mad2, is locked in the O-Mad2 conformation, is unable to form stable complexes with Mad1 or Cdc20, and elutes as a monomer from a SEC column. Together with the results in **(A)**, this shows that neither conformer of Mad2 is able to form oligomers if the opposite conformer is missing. **(C)** Stoichiometric amounts of Cdc20¹¹¹⁻¹³⁸:C-Mad2 and O-Mad2^{AC} were combined and separated by SEC. A trimeric Cdc20¹¹¹⁻¹³⁸:C-Mad2:O-Mad2 complex is formed. The presence of stoichiometric amounts of C-Mad2 and O-Mad2 in this complex is revealed by SDS-page analysis of eluted fractions thanks to the ~1 kDa difference between C-Mad2^{wt} and O-Mad2^{AC}. In summary, pure O-Mad2 or C-Mad2 samples are monomeric and form dimers when mixed stoichiometrically. We have recently suggested that the oligomerization of bacterially expressed HsMad2 is likely due to spontaneous formation of C-Mad2 in the absence of Mad1 or Cdc20, and its consequence binding to O-Mad2 (DeAntoni et al., 2005). **(D)** The SEC elution profiles of Mad2^{wt}, Mad2^{F141A} and Mad2^{R184A}. At 30 μ M, both mutants behave as monomer in solution, indicating that they are unable to form O-Mad2:C-Mad2 dimers.

Supplementary Figure 4

A model of Mad2 checkpoint regulation

(A) A Mad1:C-Mad2 complex might be recruited to the kinetochore in a complex with p31^{comet}. When p31^{comet} is bound to C-Mad2, the checkpoint is off because the pools of O-Mad2 and C-Mad2 are unable to interact. The kinetochore regulates the release of p31^{comet} from C-Mad2, possibly via a post-translational modification. (A') Binding of O-Mad2 to Cdc20 in the cytosol is kinetically disfavored. If any C-Mad2:Cdc20 forms, p31^{comet} buffers its ability to catalyze the formation of more C-Mad2:Cdc20 complexes. (B) With the inactivation of p31^{comet} at the kinetochore, O-Mad2 cycles at the kinetochore using the Mad1:C-Mad2 complex. (B') As more p31^{comet} is inactivated at the kinetochores, an autocatalytic loop based on the existing C-Mad2:Cdc20 promotes the accumulation of C-Mad2:Cdc20 in the cytosol. (C) A dynein-dependent system removes the Mad1:C-Mad2 complex from the kinetochore, halting the kinetochore-based inactivation of p31^{comet}. (C') Concomitantly, the re-activation of p31^{comet} results in the dampening of the cytosolic amplification loop. (D) An implication of the model shown in panels A-C' is that p31^{comet} binds Mad1:C-Mad2 besides Cdc20:C-Mad2. To test this hypothesis, we carried out a size-exclusion chromatography analysis using a Superdex-200 column (Amersham) on a Smart system. Pure p31^{comet} eluted in a single peak as expected for its size; (E) C-Mad2:Mad1⁴⁸⁵⁻⁵⁸⁴ also eluted from the column in a single peak. (F) p31^{comet} and C-Mad2:Mad1⁴⁸⁵⁻⁵⁸⁴ were mixed stoichiometrically, incubated at 20°C for 30' and analyzed as above. The three proteins co-eluted in a high-molecular complex, indicative of complex formation.

Supplementary References

Chenna, R., Sugawara, H., Koike, T., Lopez, R., Gibson, T.J., Higgins, D.G. and Thompson, J.D.

(2003) Multiple sequence alignment with the Clustal series of programs. *Nucleic Acids Res*, **31**, 3497-3500.

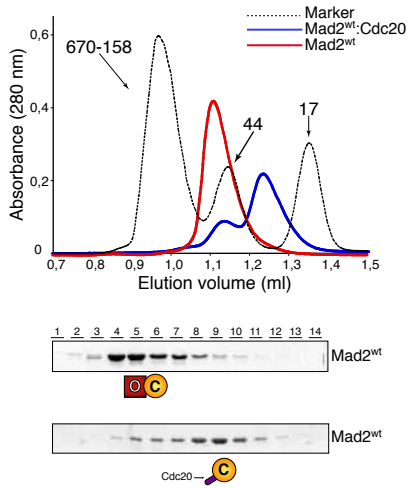
Clamp, M., Cuff, J., Searle, S.M. and Barton, G.J. (2004) The Jalview Java alignment editor.

Bioinformatics, **20**, 426-427.

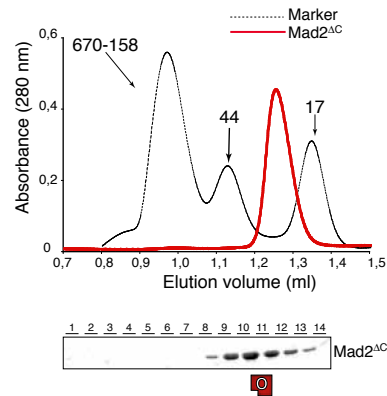
DeAntoni, A., Sala, V. and Musacchio, A. (2005) Explaining the oligomerization properties of

the spindle assembly checkpoint protein Mad2. *Philos Trans R Soc Lond B Biol Sci*, **360**, 637-647, discussion 447-638.

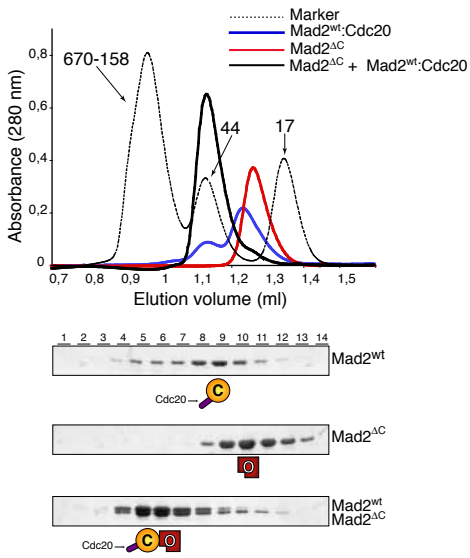
A Mad2^{wt}
Cdc20:C-Mad2^{wt}



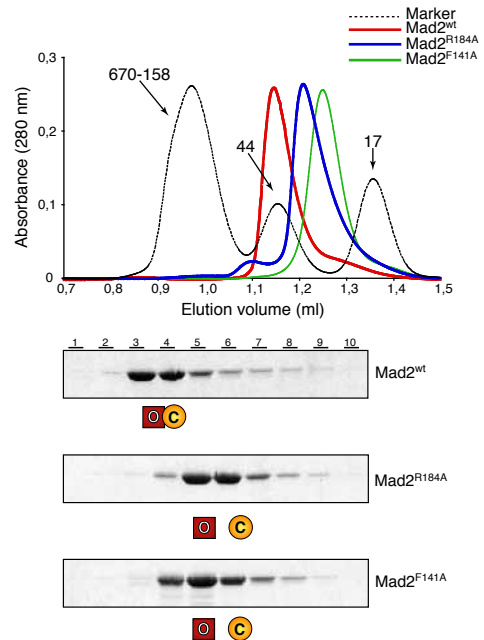
B Mad2^{ΔC}

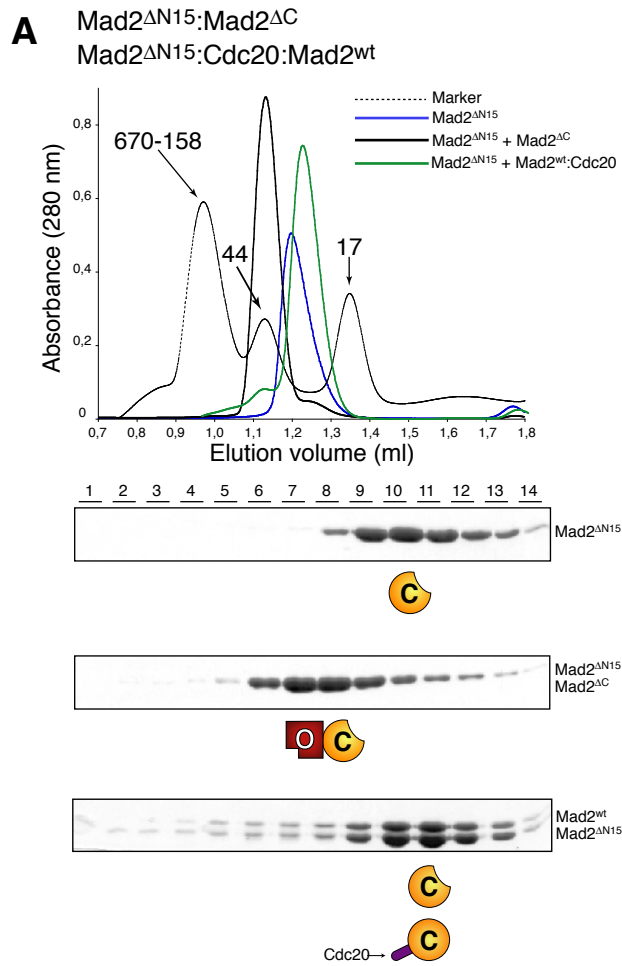


C Mad2^{wt}:Cdc20:Mad2^{ΔC}

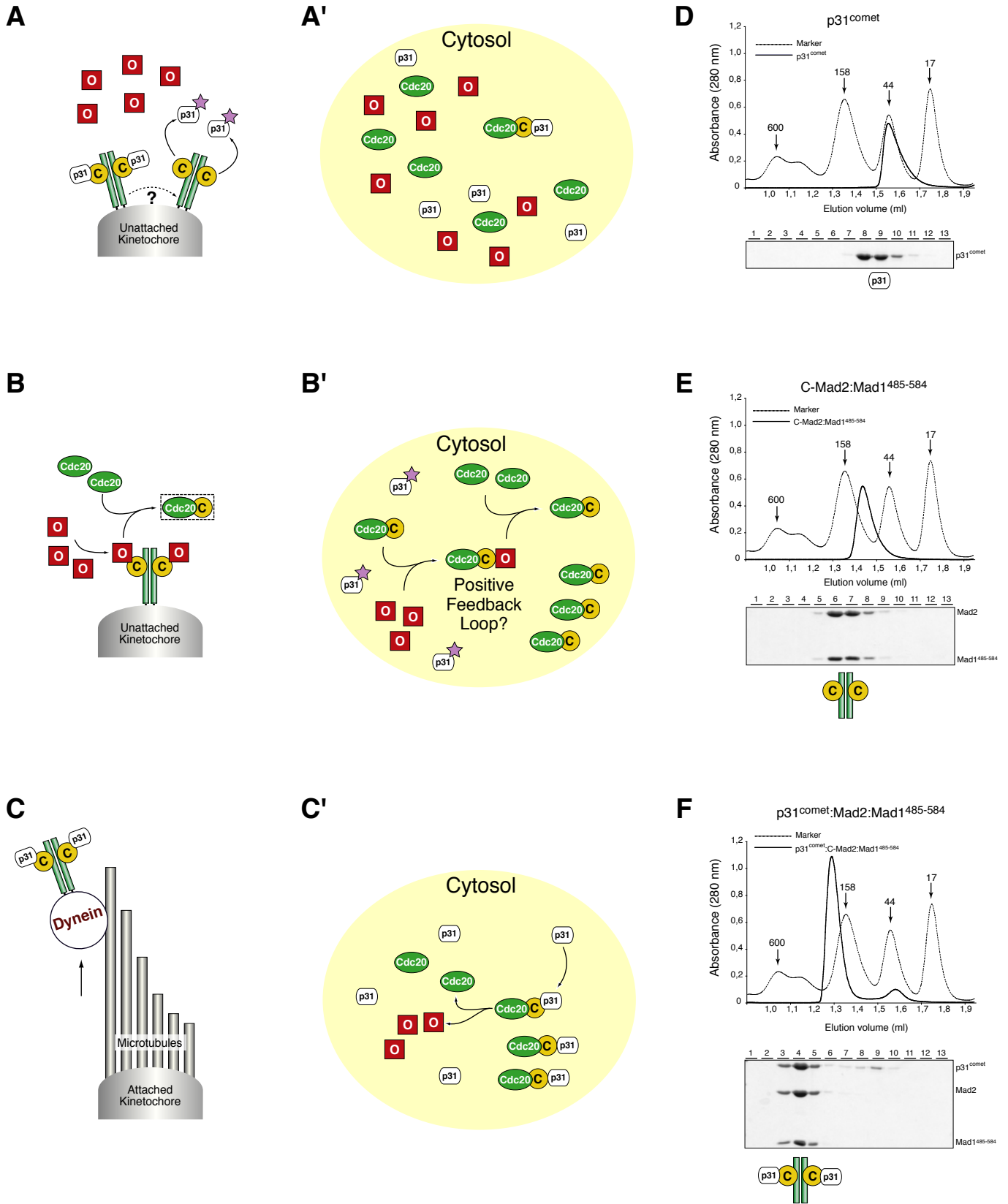


D Mad2^{wt}
Mad2^{R184A}
Mad2^{F141A}





Mapelli et al.
 Supplementary Figure 3



Mapelli et al.
Supplementary Figure 4